International Conference on Space Optics—ICSO 2014

La Caleta, Tenerife, Canary Islands

7–10 October 2014

Anamorphotic telescope for earth observation in the mid-infrared range

Thomas Peschel

Christoph Damm

Sebastian Scheiding

Matthias Beier

et al.

ANAMORPHOTIC TELESCOPE FOR EARTH OBSERVATION IN THE MID-INFRARED RANGE

Thomas Peschel[1], Christoph Damm[1], Sebastian Scheiding[1, 2], Matthias Beier[1], Stefan Risse[1], Susanne Nikolov[3], Wolfgang Holota[4], Stefan Weiß[3], Peter Bartsch[3]

[1] *Fraunhofer Institut für Angewandte Optik und Feinwerktechnik IOF, Jena, Germany,* [2] *Astro- und Feinwerktechnik Adlershof GmbH, Berlin, Germany,* [3] *EADS Astrium GmbH, Ottobrunn, Germany,* [4] *Holota Optics, Bad Tölz, Germany*

I. INTRODUCTION

In the framework of the "Earth Explorer" program, the European Space Agency had foreseen the PREMIER mission intended to monitor the three-dimensional distribution of trace gasses in the atmosphere [1].

One of the main instruments in this concept is the "Infrared Limb Sounder" (IRLS). It relies on an imaging Fourier-transform spectrometer which looks into the atmosphere at the horizon. Effectively, the instrument generates a vertical cut-view through the atmosphere (see fig. 1). In contrast to this strategy, conventional nadir-viewing instruments like those on MetOp integrate over the height distribution.
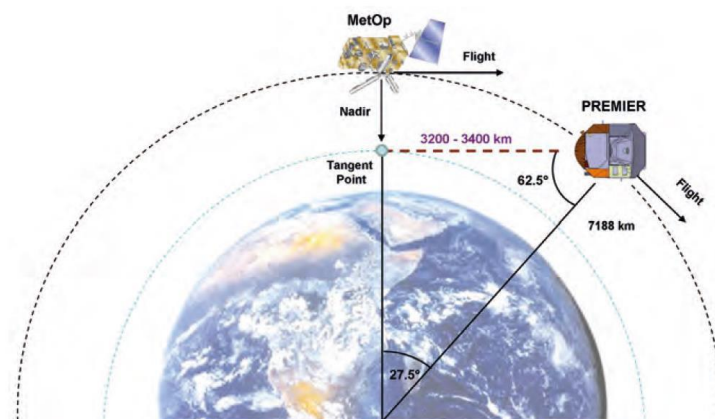

Fig. 1. Geometry of observation of the Infrared Limb Sounder [1].

The geometry of observation requires an anamorphotic telescope to transfer the rectangular field of view onto the square entrance aperture of the interferometer.

The conventional solution using a telescope with an anamorphotic add-on based on prisms or cylindrical lenses [2] would result in an excessively heavy and bulky design. To minimize the number of optical elements, the integration of the anamorphotic imaging directly into the telescope is preferred. However, this strategy dictates the need for using surfaces with large deviations from rotational symmetry.

Such freeform optical elements are difficult to manufacture [3] and require new strategies for alignment of the instrument, since 6 degrees of freedom have to be controlled for each optical element [4, 5].

To increase the technology readiness level for such a system, a demonstrator of the IRLS telescope was designed and built. The concept of the demonstrator is based on a four-mirror all-freeform optical system.

II. DESIGN OF THE TELESCOPE

A. Optical design

The anamorphic telescope relies on an afocal off-axis four-mirror design. The optical layout is depicted in fig. 2. The rectangular entrance pupil with a size of 150 mm by 25 mm can be seen on the bottom left side. All mirrors are freeforms of the so-called biconic type:

$$z(x, y) = \frac{c_x x^2 + c_y y^2}{1 + \sqrt{1 - (1 + k_x) c_x^2 x^2 + (1 + k_y) c_y^2 y^2}} + \sum_{i=2}^{5} a_i \left((1 - b_i) x^2 + (1 + b_i) y^2 \right)^i \tag{1}$$

The mirrors share two common planes of symmetry, the intersection of which corresponds to the optical axis in conventional systems. The entrance pupil of the telescope is shifted with respect to this axis and the viewing direction is slightly tilted. Hence, the used areas on the mirrors are far off the axis of symmetry.

The telescope images a field of ±3.22° in vertical and ±0.47° in horizontal directions, respectively. The corresponding magnifications are 0.5x and 3x, respectively. Orientations are given with respect to the field of view of the satellite.
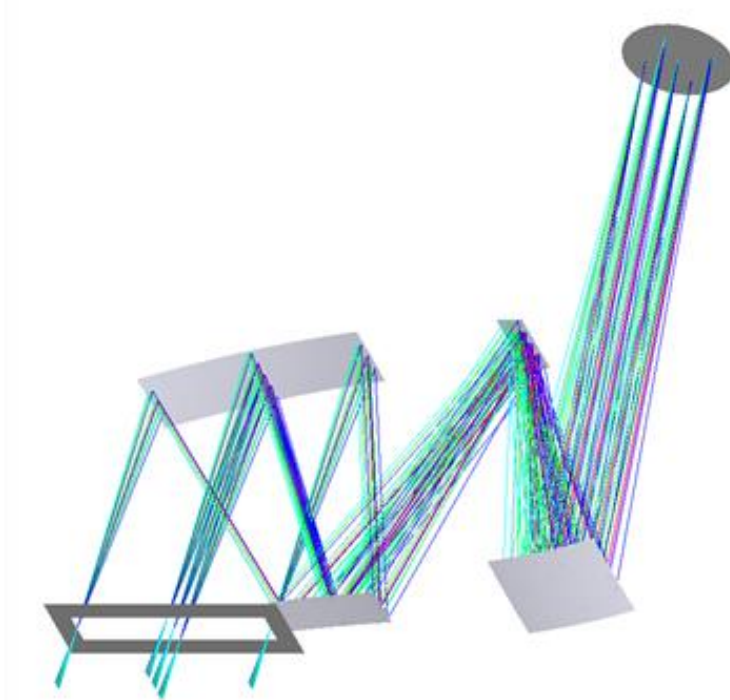

Fig. 2. Optical layout of the telescope. The entrance pupil is on the bottom left side.

The optical design yield diffraction-limited wavefront quality for the intended wavelength range of 6 to 13 µm. The required surface quality of the mirrors of 1.4 µm peak to valley is compatible with the intended fabrication approach by single-point diamond turning.

B.   *Mechanical design*

To simplify the fabrication of the mirror as well as the alignment of the telescope, the mirrors were arranged in pairs. Each pair of mirrors is fabricated in a single machining run together with the respective reference surfaces used for alignment [4]. This procedure results in an excellent knowledge of the mirror positions w.r.t. each other and to the reference features.
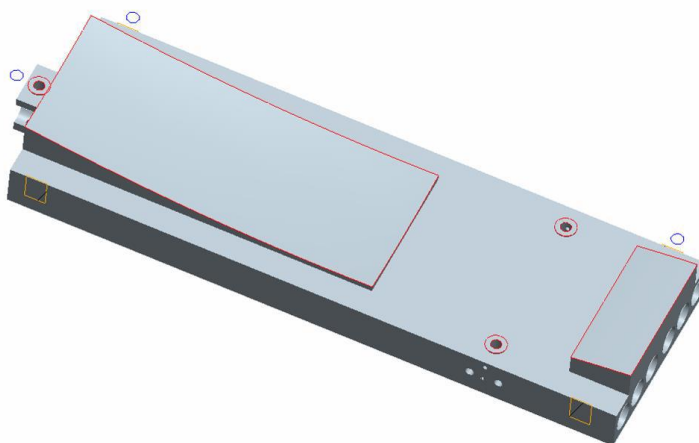

Fig. 3. Mirror subassembly M1-M3. Reference features for alignment are marked red.

The housing of the telescope is based on a light weight box design made from two shells. The mirrors were attached to the housing via kinematic mounts to prevent deformations of the housing from influencing the mirror surfaces. However, the stiff substrates of the mirror pairs have some stabilizing influence on the whole system.

To simplify alignment, the housing carries reference surfaces corresponding to those on the mirror substrates. Those surfaces are finished by single point diamond fly-cutting of the assembled housing structure.
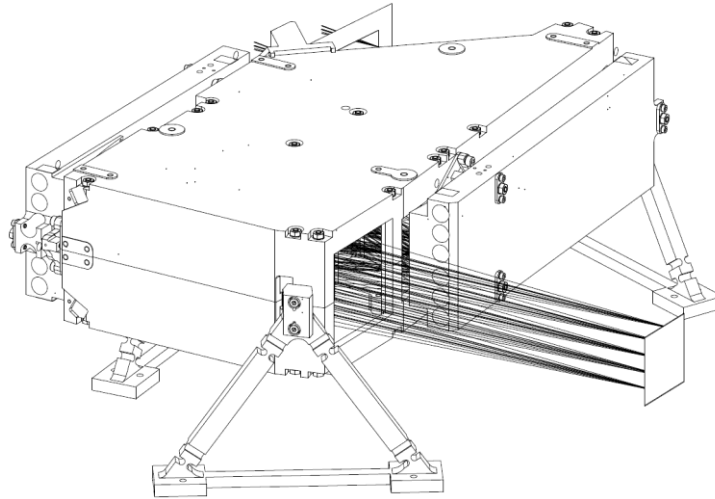

Fig. 4. Mechanical layout of the telescope. The entrance pupil is on the back side.

In order to minimize influences of planarity tolerances of the optical bench of the instrument, the whole telescope is mounted kinematically on three bipods.

The current design results in a total mass of the telescope as low as 6.3 kg. Nevertheless, the lowest resonance frequency, which is important for the stability of the telescope against vibrations, is as high as 319 Hz (see fig. 5). The corresponding deformation pattern shows that it is limited by bending of the housing in the areas of the large optical apertures.
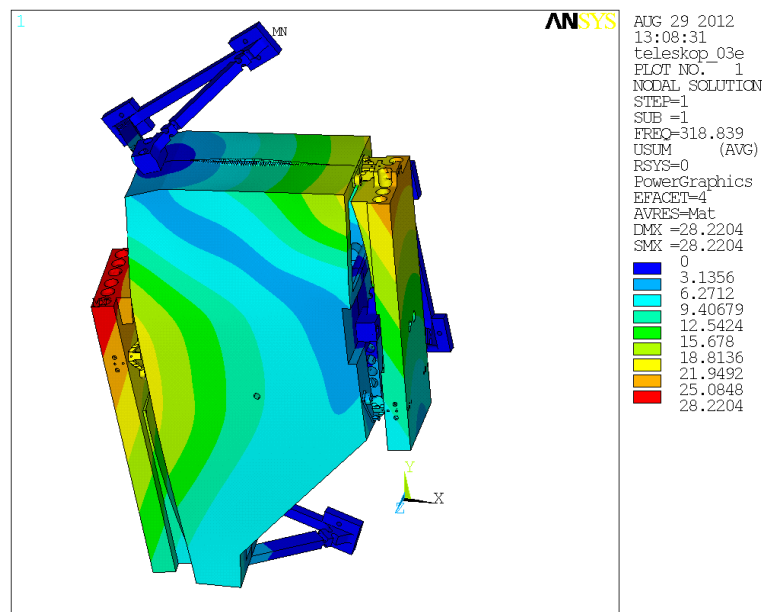

Fig. 5. Lowest Eigenmode of the telescope at 319 Hz. Colours show the corresponding displacement in arbitrary units.

Since the whole telescope is made from a single material (Al 6061 T6), an athermal behavior under variations of the ambient temperature is obtained. The response to thermal gradients is low because the thermal conductivity of the telescope housing is large compared to that of the kinematic mounts (see fig. 6).
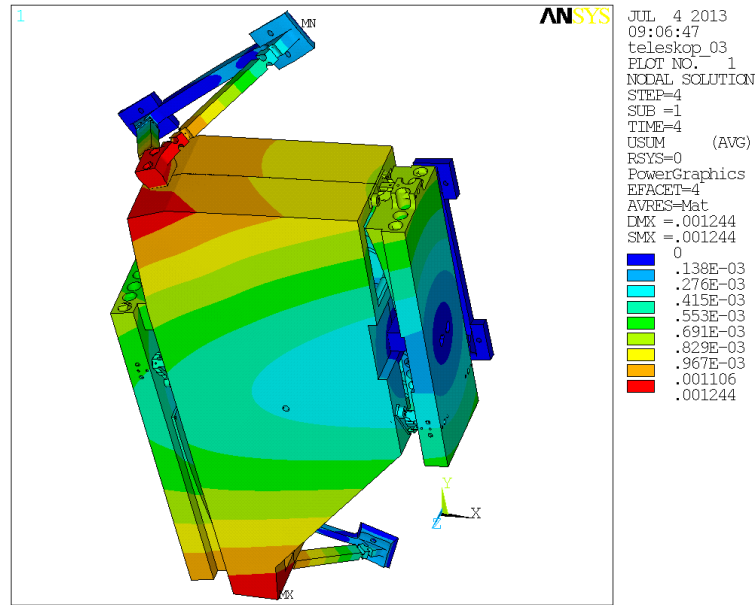
Fig. 6. Response of the telescope to a thermal gradient of 1 K in y-direction. Colours indicate the corresponding displacement in mm. The maximum value is 1.2 μm.

III. MANUFACTURING

A. *Manufacturing of the mirror pairs*

The mirrors M1/M3 and M2/M4, respectively, are machined on a common mirror substrate to bind the position and orientation of the two elements with respect to each other. The fabrication of the freeform surfaces is based on a freeform manufacturing approach using a Fast Tool Servo (FTS) system [6]. The FTS is a redundant kinematic in addition to the in-feed axis of the ultra-precision machine. The actuator is a voice coil servo with a stroke of ±3 mm. The working principle is based on the synchronous feed of the FTS slide to the angular position of the working spindle to generate the freeform shaped surface.

To fabricate two mirrors on a common substrate in a single machining process, the two surfaces have to be described as one continuous surface in a common polar coordinate system.

The center of revolution for the mirror assemblies is shifted with respect to the axis of symmetry in order to minimize the diameter of the work piece. Furthermore, the surfaces were tilted to minimize the FTS stroke which must be smaller than 6 mm.

In the next step, the resulting surface profiles were split in a rotationally symmetric and a non-symmetric part in a first step. The symmetric part is processed like a conventional asphere, i.e. by a slow motion of the support.
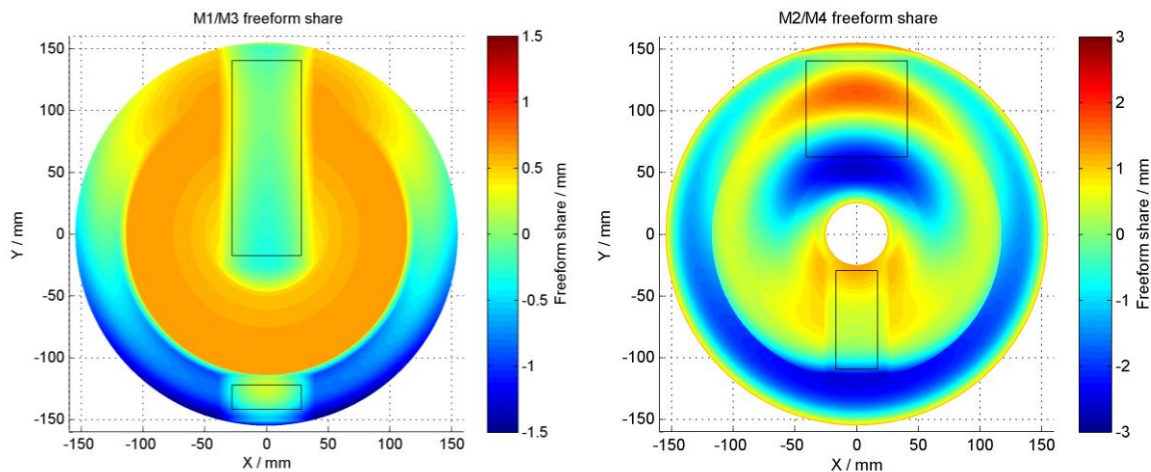

Fig. 7. Freeform part of the calculated tool paths for both mirror pairs.

Subsequent to the transformation and splitting, the surfaces are compensated for the contour radius of the diamond cutting tool to derive the tool center position. The description of the whole circular cutting surface is achieved by extrapolating the optical surfaces to a continuous surface. The freeform parts of the resulting tool paths obtained for both mirror pairs are depicted in fig. 7.

After cutting, the surface form is measured and the resulting errors are fed back into the tool path. Finally, the peak-to-valley (p.-v.) form errors of 1.2 µm and 0.6 µm could be achieved for the large mirrors M1 and M4, respectively (see fig. 8). In the case of the M1-M3 assembly, the achievable quality was limited primarily by the long processing times of 21 h. During that period, minor fluctuations of the temperature in the range of 0.2 K could not be avoided completely, which led to corresponding deviations in the positions of tool and mirror. Since such variations are not predictable, they cannot be compensated for in the correction loop.

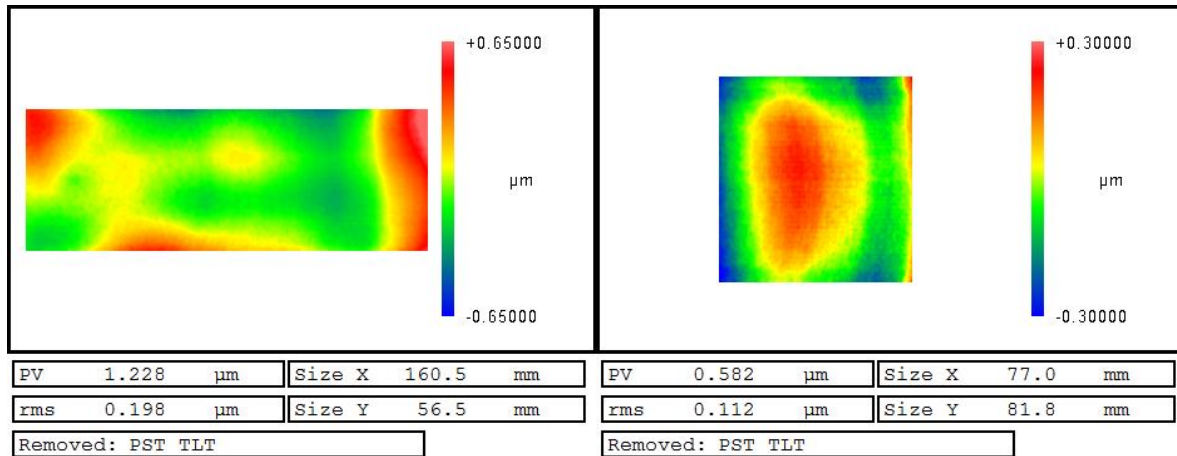The small mirrors M2 and M3 reached p.-v. form deviations of 0.4 µm.

PV	1.228	µm	Size X	160.5	mm
rms	0.198	µm	Size Y	56.5	mm
Removed: PST TLT					

PV	0.582	µm	Size X	77.0	mm
rms	0.112	µm	Size Y	81.8	mm
Removed: PST TLT					

Fig. 9. Form error of the large mirrors M1 (left) and M4 (right).

The surface roughness of the mirrors is in the range of 8.3 nm root mean square (r.m.s.) on M2 up to 12.8 nm on M3. Two main sources of roughness could be identified:

Relatively high values of the cutting speed as well as the dynamics of the FTS had to be chosen in order to keep the processing time in a reasonable range (below 24 h). In general, the surface quality decreases towards the outer edges of the mirrors. A sample of such a region is depicted in fig. 10.

Grains in the Aluminum base material were identified as the second source of roughness.
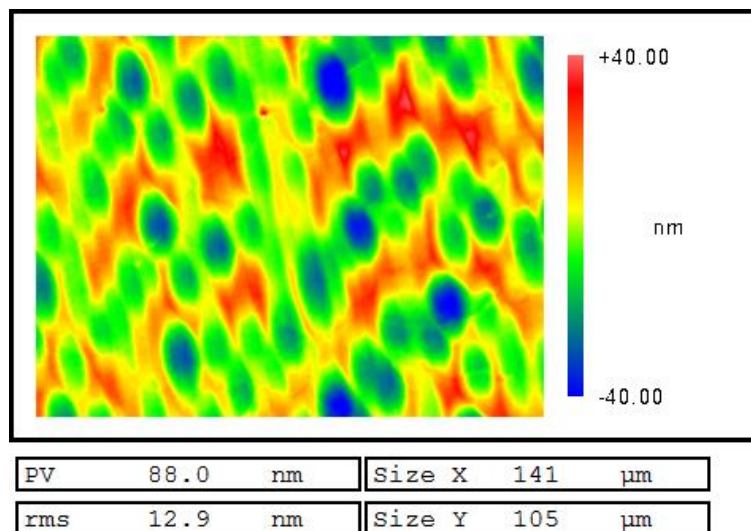
PV	88.0	nm	Size X	141	µm
rms	12.9	nm	Size Y	105	µm

Fig. 10. White light interferometry image of the micro roughness on the outer edge of mirror 1.

The interface surfaces for the alignment on the telescope housing (reference z, tilt x, tilt y) are machined in the same setup. For this purpose, an additional milling module was integrated on the tool support (see fig. 11).
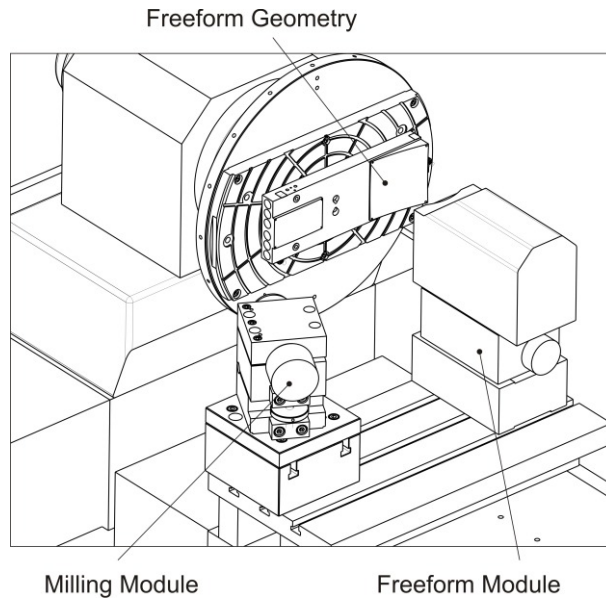
Freeform Geometry

Milling Module   Freeform Module
Fig. 11. Machining setup.

B.   Manufacturing of the telescope housing

In a first step, both halves of the telescope housing were bolted together. In the next step the positions of the reference flats of the housing were measured.

Then, the assembly was placed on a precision turntable of a single point diamond milling machine. Here, the mounting surfaces for the mirrors as well as the matching reference surfaces on the housing and the optical references were reworked to the machine precision (see fig. 12).
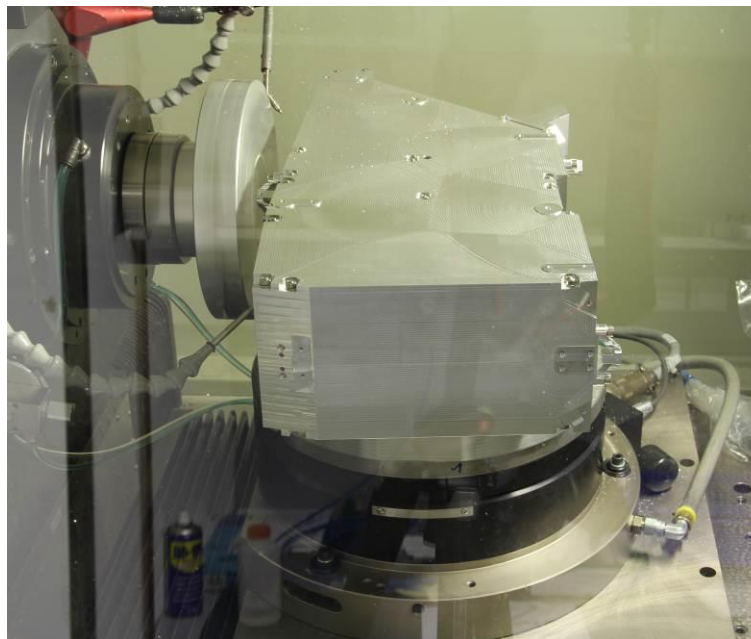

Fig. 12. Machining of the reference surfaces of the telescope housing.

IV.   INTEGRATION

The manufacturing process resulted in an excellent knowledge of the mirror positions w.r.t. each other and to the reference features. As a consequence, the preliminary adjustment of the telescope could be completed within several hours. In the next step, the telescope was placed in front of an interferometer (see fig. 13) using the reference surfaces on both sides of the entrance aperture for alignment.
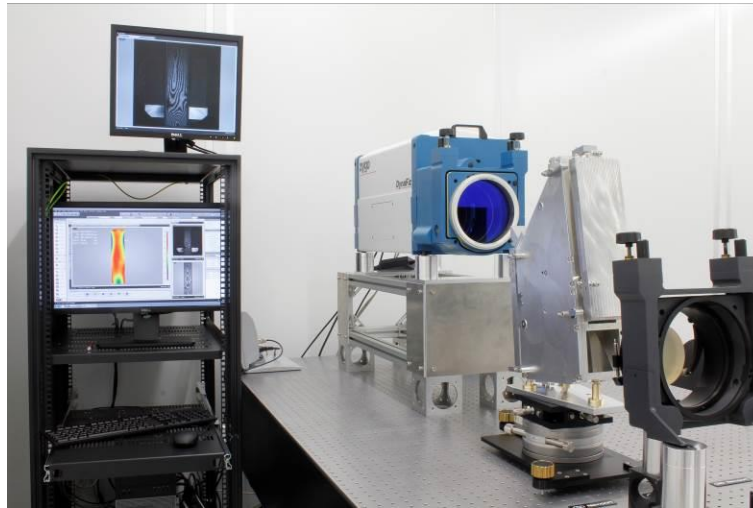
Fig. 13. Adjustment setup in front of the interferometer.

The wavefront measurement was done in an auto-collimation setup. A usable interferogram could be obtained immediately. Then, the adjustment of the mirrors was continued under interferometric control. In summary, only two iterations were needed to find the optimum mirror positions. The assembled telescope demonstrator is depicted in fig. 14.
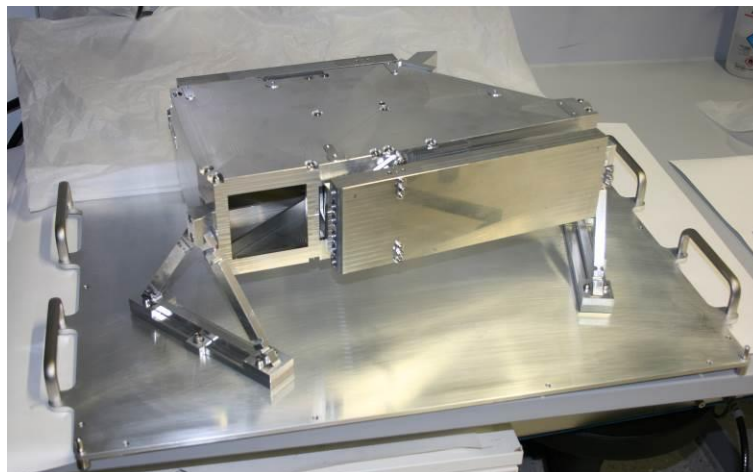

Fig. 14. Assembled telescope.

V.   TESTS AND RESULTS

The final interferometric characterization of the telescope demonstrator was performed in horizontal position, i.e. mounted on its base plate as shown in fig. 14. An auto-collimation setup was used with a plane mirror as reference.

The experiments proved a wavefront quality in the range of 300 nm to 800 nm r.m.s. depending on the position in the image field. This quality allows for diffraction-limited imaging for the intended wavelength range above 6 µm in the mid-Infrared spectral range. A summary of the measured wave front errors is given in fig. 15.

The telescope was connected to the base plate without adjustment of the bipods and using simple screws. Nevertheless, no artefacts due to the mounting could be detected, which proves the kinematic function of the bipods.
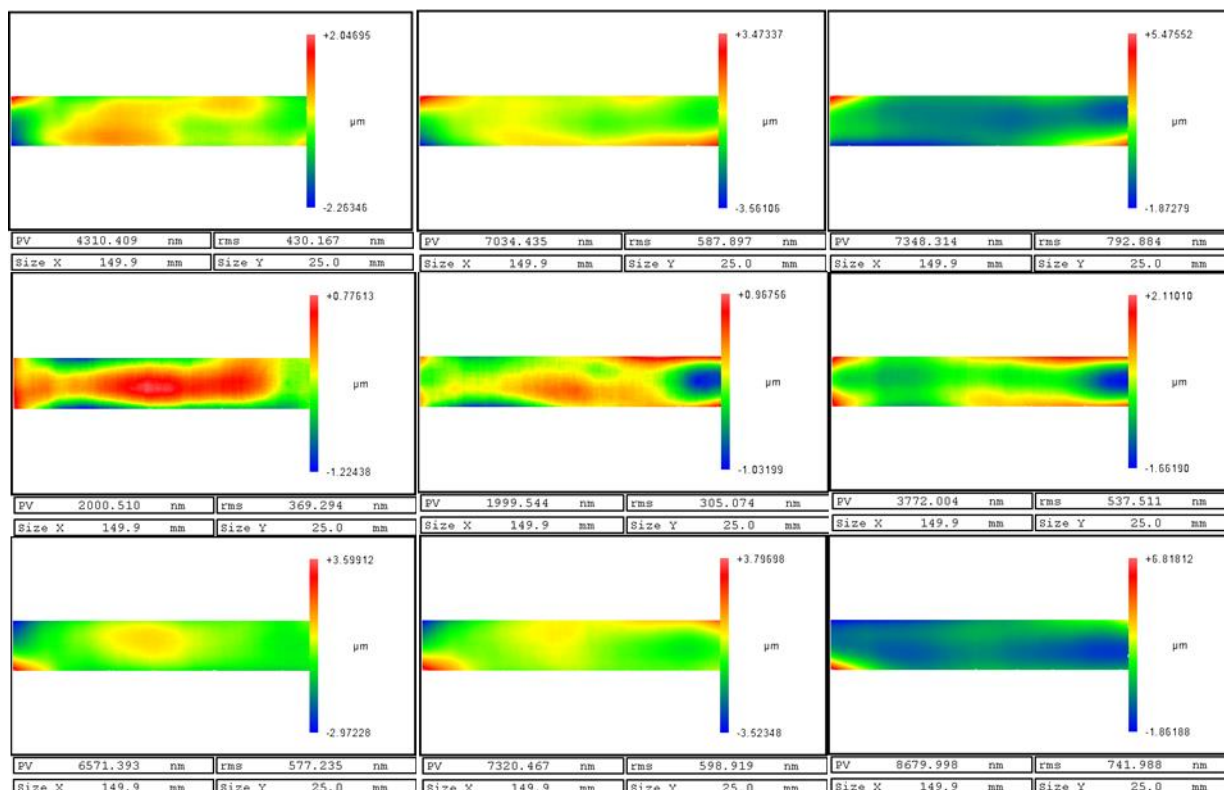
Fig. 15. Measured wave front error for nine field positions. The arrangement of the pictures corresponds to that of the field points. Piston and tilt were removed.

VI.   CONCLUSIONS

The demonstrator of the PREMIER telescope could be assembled and adjusted successfully. Reference features and mounting areas on the mirror substrates were used, which were produced without removing the mirrors from the machine. This strategy has proven to be successful. An interferometric result could be obtained immediately after assembly and adjustment turned out to be straight forward.

The achievable quality of the mirrors was limited only by the thermal stability of the machine over the processing time needed. However, diffraction limited imaging performance could be demonstrated for the mid-infrared spectral range.

To further improve the shape as well as the roughness of the mirrors, an additional polishing layer might be applied. Typical materials are chemically deposited Nickel or amorphous Silicon. After diamond turning, this layer can be further processed by conventional polishing. Surface shapes below 150 nm p.-v. as well as roughness values below 1 nm r.m.s. have been demonstrated [7].

VII.   REFERENCES

[1]   European Space Agency, "Report for Mission Selection: PREMIER", ESA SP-1324/3 (3 volume series), Noordwijk NL, 2012. Available at http://esamultimedia.esa.int/docs/EarthObservation/SP1324-3_PREMIER.pdf.
[2]   H. Paul ed., *"Lexikon der Optik"*, Berlin, 1999 (in German).
[3]   R. Steinkopf, S. Scheiding, A. Gebhardt, S. Risse, R. Eberhardt, A. Tünnermann, "Fly-cutting and testing of freeform optics with sub-µm shape deviations", *Proc. SPIE 8486*, 84860K, 2012.
[4]   S. Scheiding, C. Damm, W. Holota, T. Peschel, A. Gebhardt, S. Risse, A. Tünnermann, "Ultra-precisely manufactured mirror assemblies with well-defined reference structures", *Proc. SPIE* 7739, 773908, 2010.
[5]   S. Risse, S. Scheiding, A. Gebhardt, C. Damm, W. Holota, R. Eberhardt, A. Tünnermann, "Development and fabrication of a hyperspectral, mirror based IR-telescope with ultra-precise manufacturing and mounting techniques for a snap-together system assembly", *Proc. SPIE 8176*, 81761N, 2011.
[6]   Moore Nanotechnology Systems, LLC, *"NFTS-6000 Specification Overview"*, 2013.
[7]   R. Steinkopf, A. Gebhardt, S. Scheiding, M. Rohde, O. Stenzel, S. Gliech, V. Giggel, H. Löscher, G. Ullrich, P. Rucks, A. Duparre, S. Risse, R. Eberhardt, and A. Tünnermann, "Metal mirrors with excellent figure and roughness", *Proc. SPIE 7102*, 71020C–71020C–12, 2008.